

Atomic force microscopy of supported planar membrane bilayers

Seema Singh and David J. Keller

Department of Chemistry, University of New Mexico, Albuquerque, New Mexico 87131

ABSTRACT Membrane bilayers of dipalmitoyl phosphatidylcholine (DPPC) and dipalmitoyl phosphatidylethanolamine (DPPE) adsorbed to a freshly cleaved mica substrate have been imaged by Atomic Force Microscopy (AFM). The membranes were mounted for imaging by two methods: (a) by dialysis of a detergent solution of the lipid in the presence of the substrate material, and (b) by adsorption of lipid vesicles onto the substrate surface from a vesicle suspension. The images were taken in air, and show lipid bilayers adhering to the surface either in isolated patches or in continuous sheets, depending on the deposition conditions. Epifluorescence light microscopy shows that the lipid is distributed on the substrate surfaces as seen in the AFM images. In some instances, when DPPE was used, whole, unfused vesicles, which were bound to the substrate, could be imaged by the AFM. Such membranes should be capable of acting as natural anchors for imaging membrane proteins by AFM.

INTRODUCTION

Many cellular functions which are crucial to the operation of living cells occur at cell membranes, and are mediated by membrane-bound proteins. Despite the importance of these processes relatively little is known about the structure of membrane proteins because, in general, they cannot be crystallized, and hence cannot be studied by x-ray crystallography¹ (1). One alternative is Transmission Electron Microscopy (TEM), but this approach has three disadvantages: (a) the resolution obtained is usually too low to allow reconstruction of the tertiary structure of membrane proteins, (b) electron microscopy usually requires that the samples be stained, fixed, and placed in high vacuum, thus introducing unknown distortion of structure² (2), and (c) the real-time behavior of proteins is difficult or impossible to follow.

Recently several new high resolution microscopes which have potential to overcome these drawbacks have been invented. Collectively they are known as scanning probe microscopes. The two best developed examples are the Scanning Tunneling Microscope (STM) and the Atomic Force Microscope (AFM). Both the STM and AFM can have very high resolution (3, 4), can form images of samples in ionic solutions (5, 6), and, at least in principle, can follow the reactions of biological molecules in real time (7). Scanning probe microscopes work by scanning a very sharp probe tip over the sample

surface, creating a profile image. They differ from each other only in the mechanism by which the probe tip detects the sample surface and hence forms the image. The STM works by measuring a small tunneling current between the sample and the probe tip, and so requires a conductive sample. The AFM works by measuring a tiny force of contact between the tip end and the sample surface, and so can form images of nonconducting samples (8). The operation of the AFM is essentially identical to that of a classical profilometer; the new aspects are that the AFM has a very sharp tip (for high resolution) and can measure very small forces (so soft samples may be imaged).

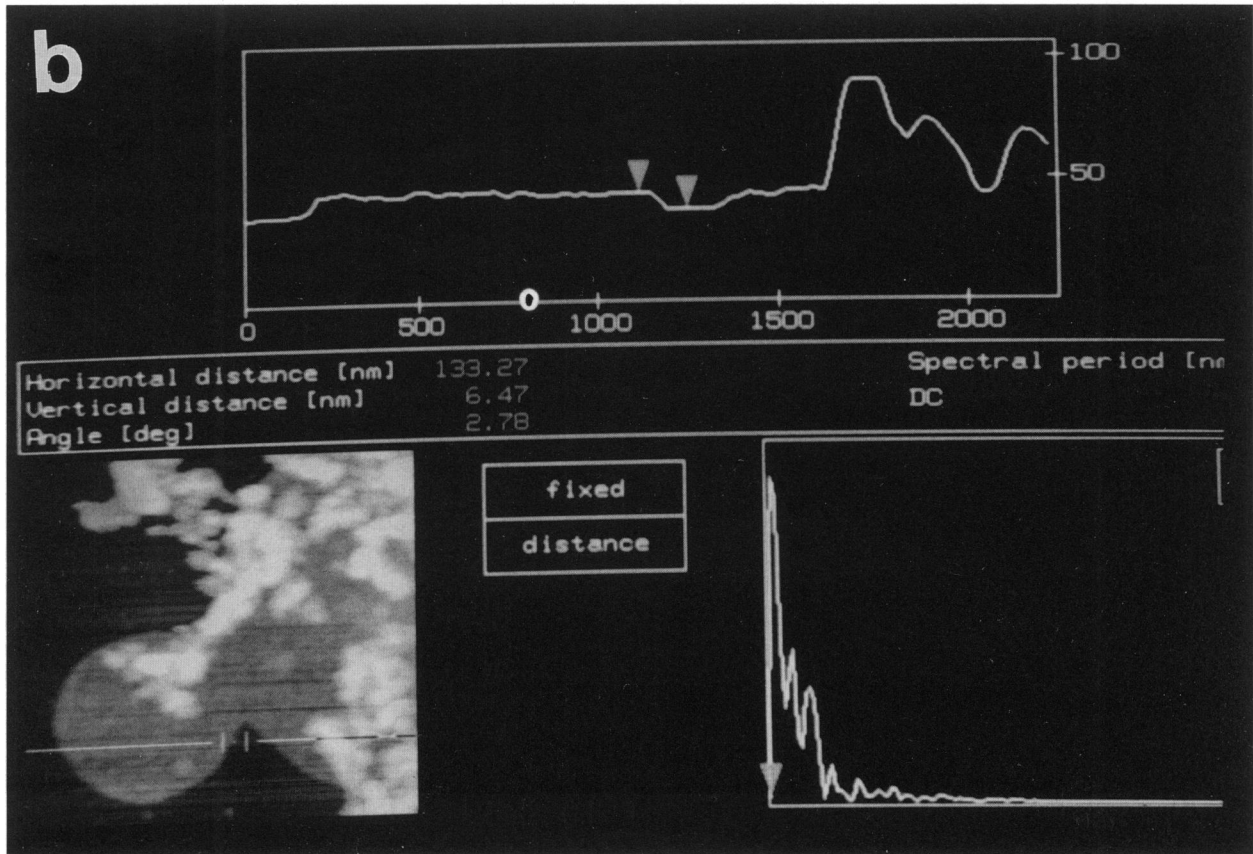
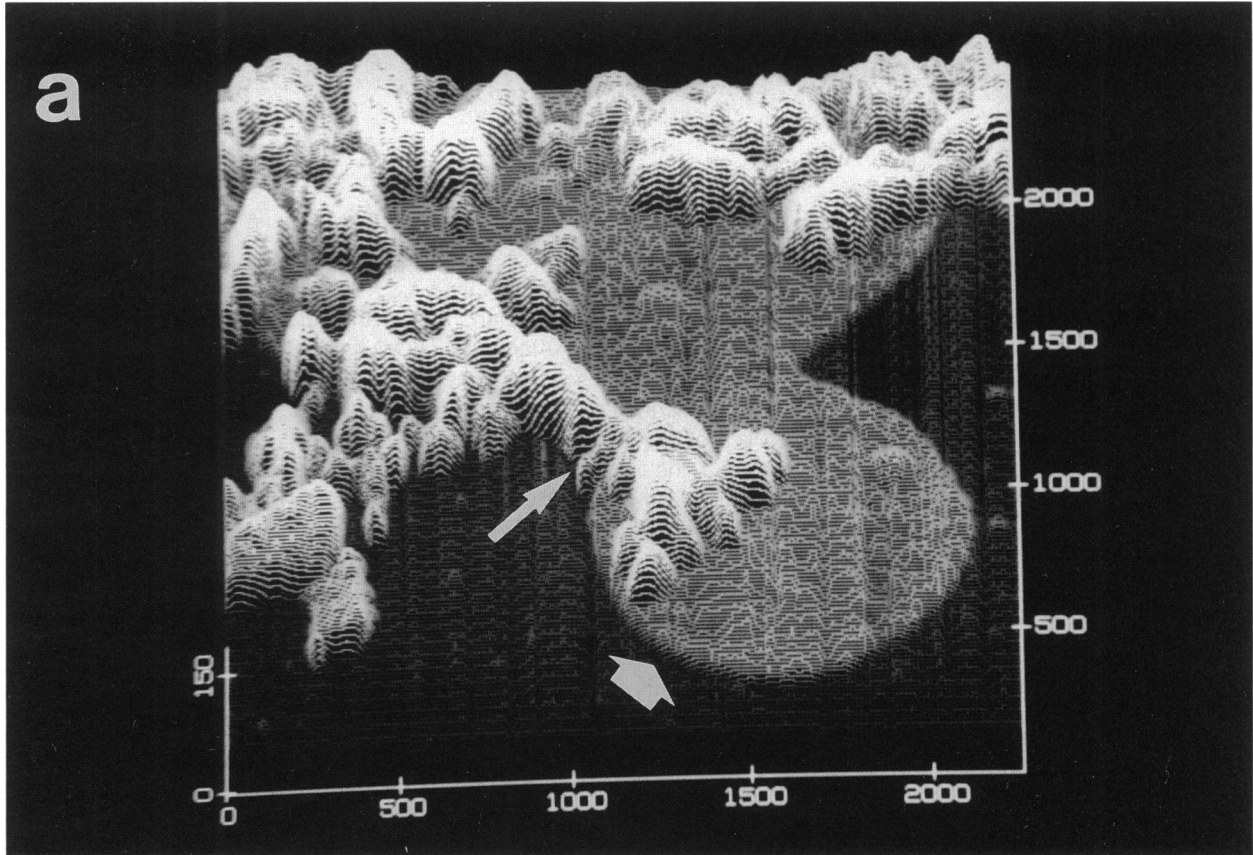
Microscopes like the AFM work best on samples which are relatively flat, and do not work well on samples with highly convoluted or recursive surfaces. Cell membranes, which can be quite flat with only low aspect-ratio features, are the type of sample the AFM works well on.

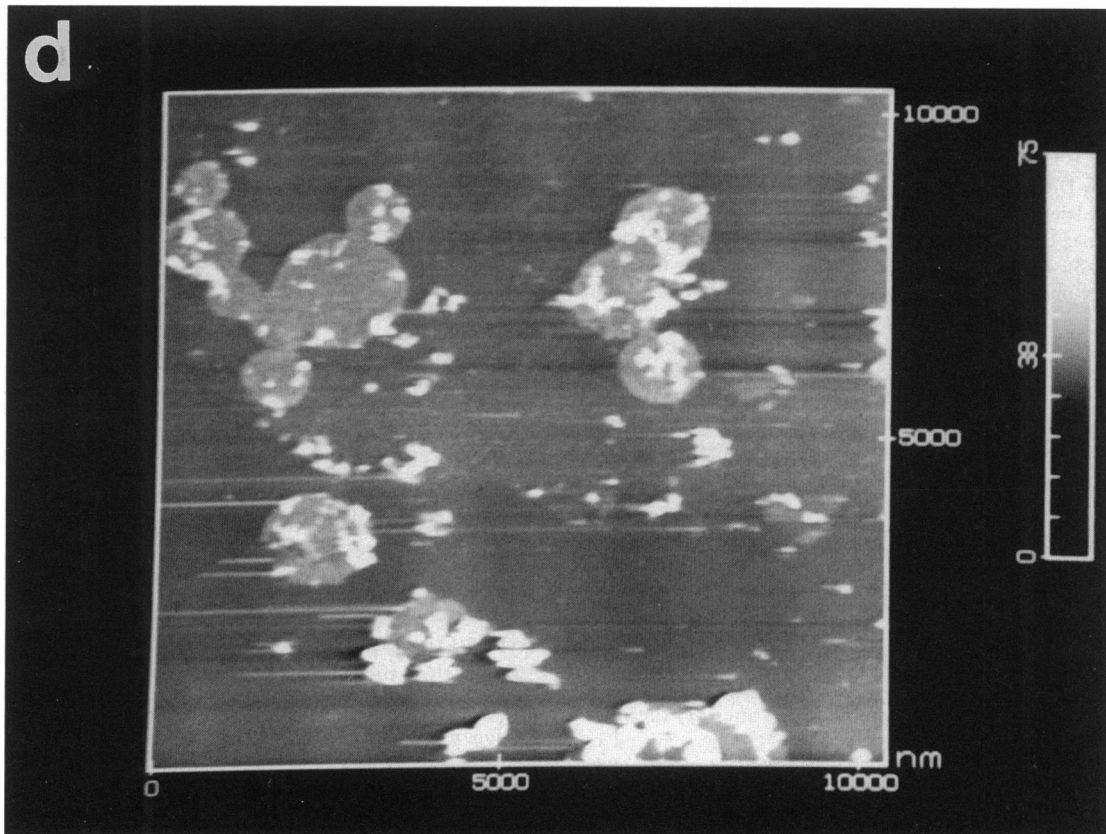
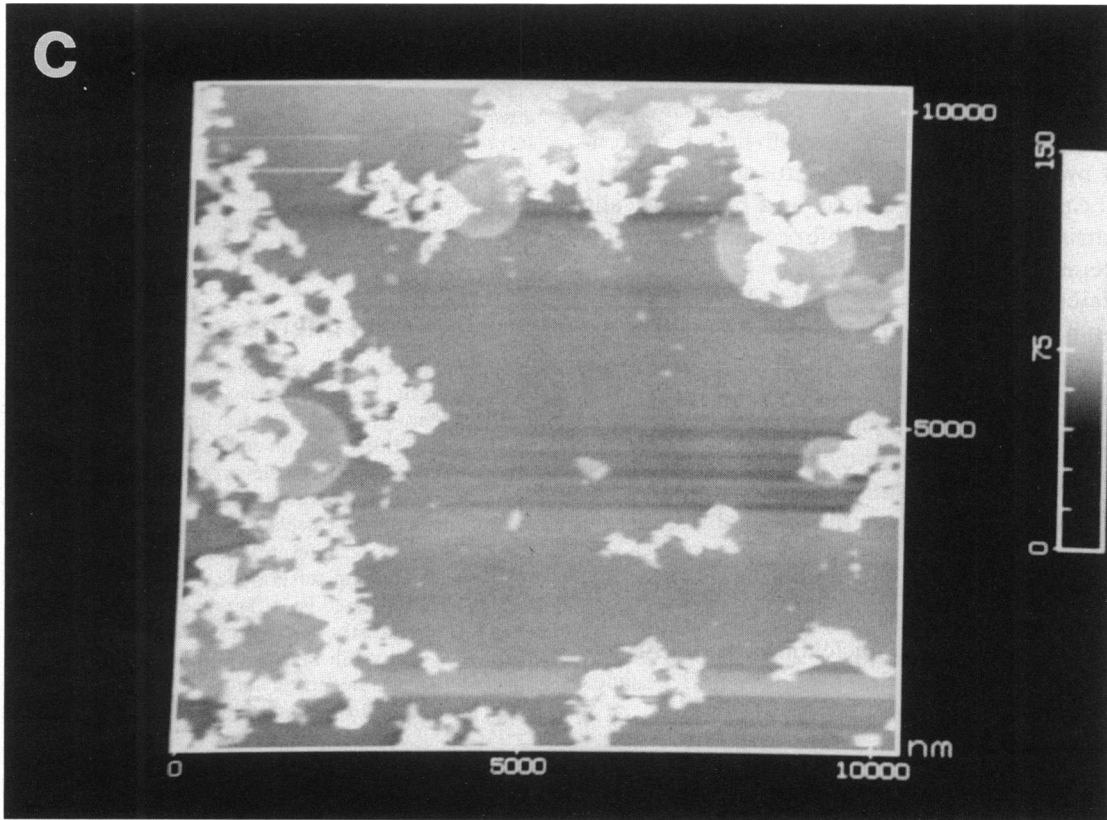
Several membrane and membrane-like systems have been imaged by AFM. For example, fragments of the purple membrane of *Halobacterium halobium* were imaged in two independent experiments (9, 9a, 10), and showed the characteristic two-dimensional crystalline pattern of bacteriorhodopsin molecules expected of this highly ordered system. Egger et al. (11) obtained AFM images of a lipid layer deposited by Langmuir-Blodgett techniques on an alkylated mica substrate. In this experiment antibody fragments were also attached to the membrane and imaged by AFM.

Here, we report the deposition of supported lipid bilayers onto mica substrates by two passive adsorption

¹There is one famous example where membrane proteins have been crystallized, namely the proteins of the photosynthetic reaction center of *R. viridis*.

²One exception to this is cryo-electron microscopy.





methods, and their imaging by AFM. A supported bilayer is an artificially prepared model cell membrane that has been adsorbed to a planar solid support. Such bilayers can be composed of a single pure lipid or can be prepared as artificial cell membranes with known concentrations of proteins and other constituents (12, 13). In the second case, the bilayer can act as a physiologically natural matrix in which to immobilize and study membrane proteins.

Two related methods are described by which lipid bilayers can be deposited on mica and imaged by AFM, and two types of membranes have been imaged: bilayers formed of dipalmitoyl phosphatidylcholine (DPPC), and vesicles formed of dipalmitoyl phosphatidylethanolamine (DPPE). It is found that the AFM can image either type of membrane without damage under normal imaging conditions. Depending on the type of deposition used, DPPC has been seen either in continuous sheets on a flat mica substrate or in symmetrical islands apparently formed by the slow "crystallization" of the lipid onto the surface from a nucleation site. DPPE has so far been seen only in the form of lipid vesicles adhered to the substrate.

MATERIALS AND METHODS

Supported planar lipid bilayers on mica or glass substrates were prepared in two ways: (a) by dialyzing a detergent solution of lipid in the presence of the substrate, and (b) by exposing the substrate to a previously dialyzed suspension of lipid vesicles.

Formation of planar membranes

L- α -DPPE, L- α -DPPC, *N*-(7-nitro-2-1-3-benzoxadiazol-4-yl) dimyristoyl phosphatidylethanolamine (NBD-DMPE), cholesterol (Avanti Polar Lipids, Inc., Birmingham, AL), and sodium deoxycholate (Sigma Chemical Co., St. Louis, MO) were obtained commercially and used without further purification. Detergent solutions were prepared and dialysis carried out by the method of Brian and McConnell (13). Chloroform solutions of lipid with 1% (mol/mol) fluorescent probe (NBD-DPPE) were dried under vacuum and dissolved in detergent-containing Tris buffer (0.5% (wt/vol) deoxycholate in 140 mM NaCl, 10 mM Tris, pH 8) by sonicating to clarity in a bath sonicator. In the first deposition method, small pieces of freshly cleaved mica were

FIGURE 1 (a) Topographical AFM image of DPPC bilayers deposited on mica by detergent dialysis, shown in three-dimensional projection. The high, sharp features (*thin arrow*) are identified as salt crystals, and the low, flat regions as adsorbed DPPC domains (*thick arrow*). Image taken in air, cantilever force constant ~ 0.6 N/m, net tip force ~ 15 nN repulsive, scan speed $19 \mu\text{m/s}$. (b) Cross-sectional profile of the bilayer, showing a typical value of the layer thickness. (c and d) Images of similar regions of the substrate before (c) and after (d) rinsing in distilled water. The sharp, high structures are largely removed by water rinsing, consistent with their identification as salt crystals. Cantilever force constant ~ 0.6 N/m, net force ~ 15 nN, scan speed $90 \mu\text{m/s}$.

placed into the detergent/lipid solution and dialyzed against four, 1 liter changes of Tris buffer for a total of 84 h at 4°C. The mica pieces were then removed from solution and allowed to air dry.

In the second method, the detergent/lipid solution was dialyzed as described above to form a vesicle suspension, and a drop of this suspension was placed on freshly cleaved mica and allowed to stand for 15–30 min. The excess solution was then removed with a corner of a filter paper, and the sample allowed to dry in air. It was found that formation of the bilayer is sometimes enhanced by rolling the droplet of vesicle suspension over the substrate surface.

Atomic force microscopy

All atomic force images were taken with a commercial AFM (Nanoscope II; Digital Instruments, Inc, Santa Barbara, CA) using commercial silicon nitride cantilevers with pyramidal tips (Nanoprobes). The force constant (force per unit deflection of the cantilever) is calculated from a knowledge of the cantilever composition and geometry (Weisenhorn, A., unpublished results). The forces used in a given imaging experiment are then calculated using these force constants and the measured average cantilever deflection. All AFM images were taken in air in the constant force mode, with a net repulsive force. Some images were processed by background subtraction, and in one image (Fig. 1 a) scan streaks were removed by replacing the spurious image lines (four in all) with values interpolated from adjacent data points. Thickness measurements on lipid layers were made directly from the AFM images and are quoted as "mean \pm standard deviation."

Epifluorescence microscopy

Epifluorescence images were taken with a Nikon inverted microscope equipped for epifluorescence imaging, using a $100\times$ long-working-distance objective. Samples were prepared by placing thinly cleaved sections of lipid-coated mica on a microscope slide, immersing in a droplet of Tris buffer containing 1% mercaptoethanol (to suppress bleaching of the NBD fluorophore), gently placing a glass coverslip on top, and sealing with nail polish.

RESULTS AND DISCUSSION

1. DPPC deposited by dialysis in the presence of cleaved mica

In the first method of deposition, pieces of freshly cleaved mica are placed in the presence of a detergent solution of lipid as the detergent is slowly dialyzed away. In this case structures similar to those in Fig. 1 are created on the mica surface.

Two types of features are visible in Fig. 1 a: high, sharp structures (*thin arrow*), and low, flat, circular "pancake" structures (*thick arrow*). Fig. 1 b is a cross-sectional profile of one of the pancake regions, showing (a) that the pancake structure has a quite uniform height above the substrate, (b) that the pancake region is somewhat rougher than the substrate, and (c) a representative value of the thickness of the layer. The average thickness is $79 \pm 11 \text{ \AA}$, as measured by averaging over all heights in rectangular regions on the layer and on the substrate and then subtracting. Fig. 1, c and d show two

similar patches of the same sample before and after it was rinsed thoroughly with distilled water. The sharp, high structures are noticeably reduced by rinsing. Rinsing also reduces the apparent layer thickness to $63 \pm 9 \text{ \AA}$.

Based on these observations we identify the pancake structures as regions of deposited lipid and the high, sharp structures as salt crystals. The measured thickness of the layers is consistent with a DPPC bilayer ($40\text{--}55 \text{ \AA}$ depending on method of measurement and the thermodynamic state of the membrane [14]) coated with a thin layer of salt. The increased roughness in the bilayer regions is most likely due to a layer of strongly adsorbed salt on the highly polar bilayer surface. The decrease in apparent bilayer thickness upon rinsing is then due to the removal of some of this salt.

The circular shape of the bilayer patches suggests two possible mechanisms for their deposition: (a) monolamellar lipid vesicles first form in solution and then burst on the substrate surface, or (b) lipid islands are deposited onto the substrate directly from solution by first forming a nucleation site and then growing radially outward. The latter mechanism seems more likely for the following two reasons: (a) the lipid patches show no sign of unevenness about their edges such as would be expected when a preformed vesicle bursts on the surface, and (b) in many cases the circular patches overlap and fuse with each other. If this were to happen by the bursting of vesicles a double bilayer would occur in the overlap region, which has never been observed. The double bilayer (or the unevenness caused by the bursting of vesicles) could eventually anneal itself out, but then the extra lipid material would be expected to spread out into the neighborhood of the overlap. The actual structures are perfectly fused circular disks, and show no sign of any extra lipid in the overlap region. In the second mechanism smooth, well equilibrated structures would be expected, and this is what is observed.

2. DPPC deposited by adsorption from vesicle suspension

In the second method of deposition the substrate is exposed to a suspension of lipid vesicles for a few minutes. In this time the vesicles fuse with the substrate. It is found by epifluorescence imaging that quite large, uniform patches of DPPC bilayer can be formed on mica by rolling the droplet of vesicle suspension over the substrate. AFM images of a sample prepared in this way are shown in Fig. 2. There is now no sign of the circular patches seen in Fig. 1. Instead, as in the epifluorescence images, there is a nearly uniform surface broken only by scattered salt crystals (Fig. 2 a, *thick arrow*) and small cracks (Fig. 2 a, *thin arrow*). Cross-sectional measurements show the wider cracks to be up to 60 \AA deep, in

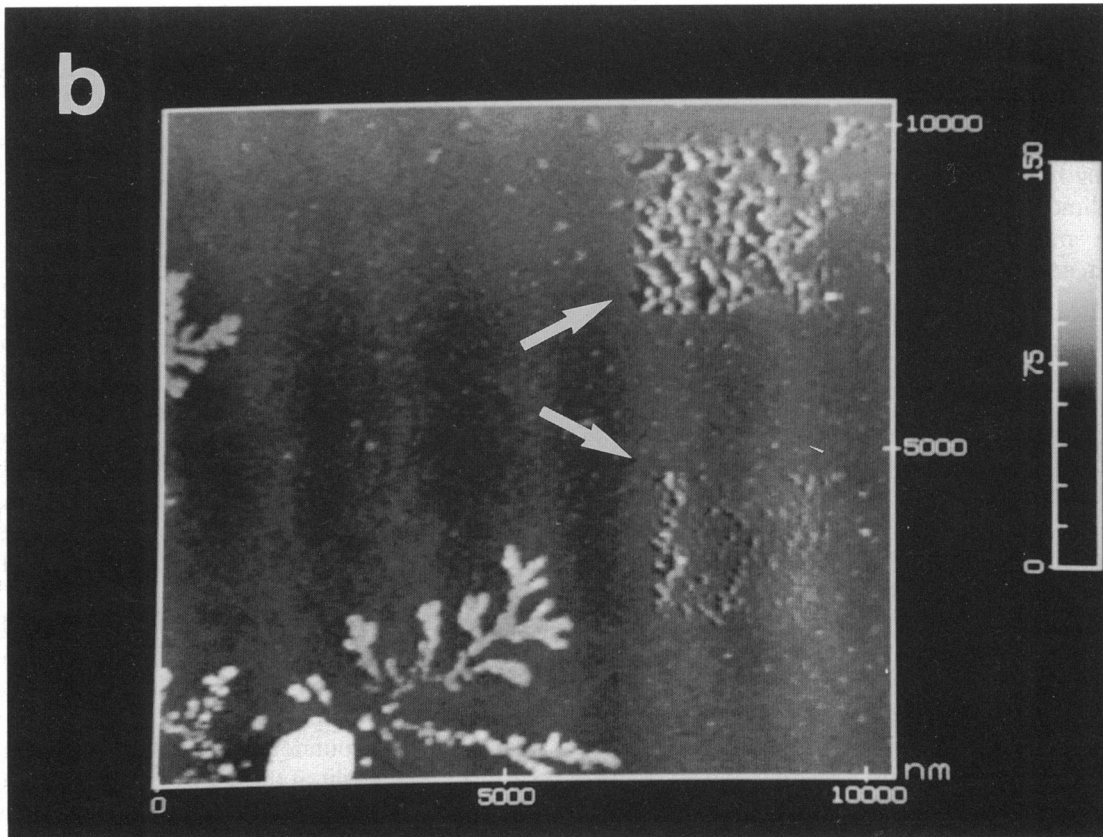
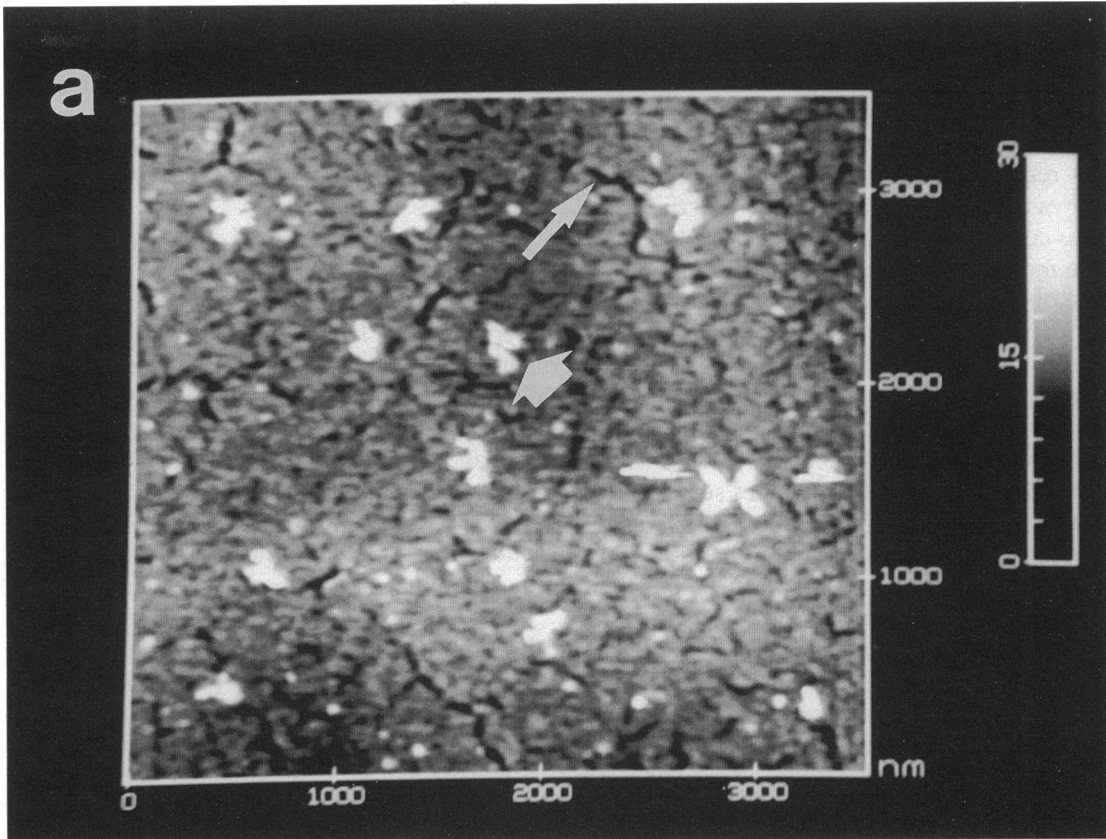
agreement with the measurements made on dialysis-deposited bilayers. The narrower cracks appear shallower, presumably because the fairly wide AFM probe tip does not touch bottom. The presence of the cracks may be due either to the drying process or to stress in the bilayer film created during the “rolling droplet” deposition.

Fig. 2 b shows the result of an experiment to see if the membrane could be damaged by the AFM probe. The two square patches in the upper and lower right (*arrows*) were created by scanning the probe over a patch of surface at relatively high, repulsive tip-sample force ($\sim 10 \text{ nN}$ more than normal) for up to 30 min, then lowering the force and widening the scan to view the damage. It was possible to create “roughened” patches like these at will. However, when a similar patch was scanned at low force for the same length of time and under the same conditions no damage occurred, showing that the membrane is stable under AFM imaging conditions. (In fact, a region in the upper center of Fig. 2 b was scanned at low force but is not visible because no damage was done.) Fig. 2 c is a higher magnification view of one of the damaged patches. The sites of damage appear to be small tears in the membrane sheet (*thick arrow*), with the torn flap of membrane folded back to one side of the hole (*thin arrow*). Salt crystals in the damaged regions have also been removed. Measurements of the depth of the holes are consistent with the rips being one membrane bilayer in thickness ($\sim 60 \text{ \AA}$). Because the substrate is entirely coated with lipid, it is not possible to tell by AFM if there is one membrane bilayer or several on the surface. Epifluorescence images show only one bilayer in most regions.

3. DPPE vesicles deposited by adsorption from vesicle suspension

When a deposition method similar to the one in the previous section was used with a vesicle suspension of DPPE, images like the ones in Fig. 3 a resulted. The dominant features in this image are large circular disks up to $\sim 2 \text{ \mu m}$ in diameter and several thousand angstroms high. The lipid suspension used for these experiments had been aged for several months at 4°C , and epifluorescence microscopy showed that large vesicles (up to several microns) had formed, and tend to adhere to mica or glass surfaces.

We therefore identify these features as DPPE vesicles that have adsorbed intact to the mica surface. Surrounding each vesicle is a rime of salt crystals. Fig. 3 b is a cross-section of a prominent vesicle, showing that it is flattened, with rounded edges and a slightly curved top surface. The height of the larger vesicles is 1,000 to 2,000 \AA . Fig. 3 c is an image of a second sample in which the



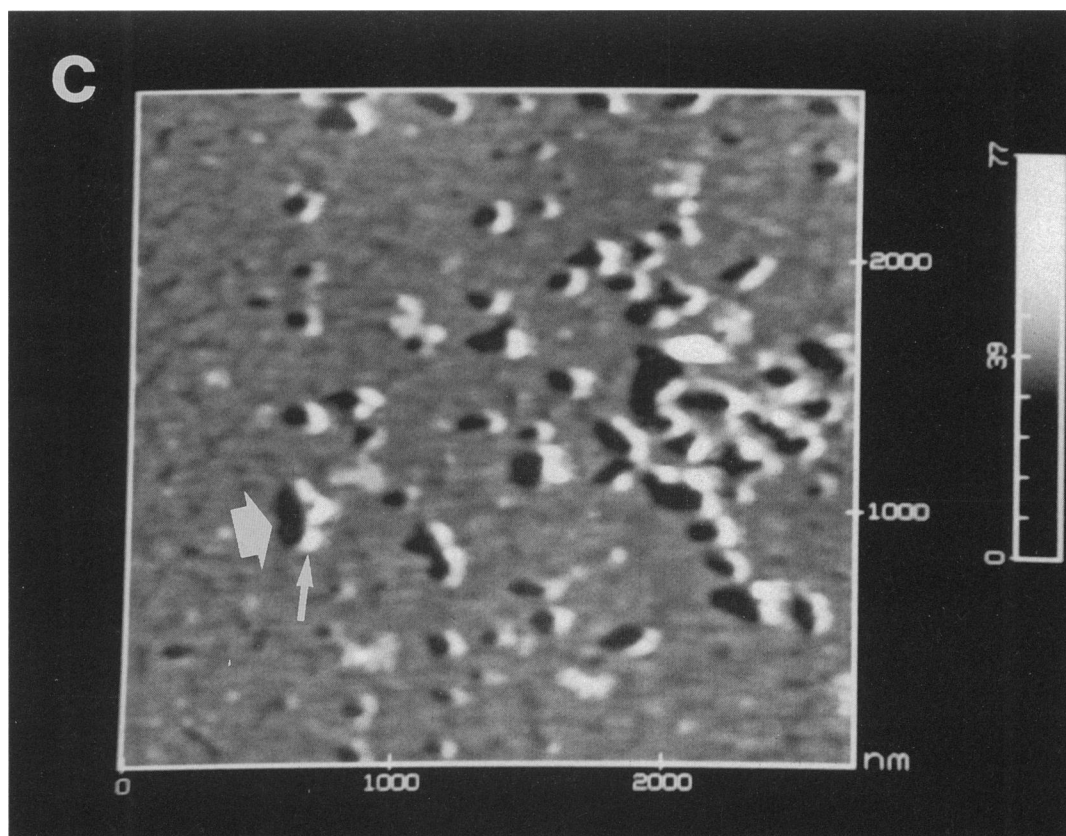


FIGURE 2 (a) Topographical AFM image of a DPPC layer deposited on mica by adsorption from vesicle suspension. Salt crystals (*thick arrow*) and cracks in the bilayer (*thin arrow*) are visible. Image taken in air, cantilever force constant ~ 0.6 N/m, net force ~ 15 nN, scan speed $30 \mu\text{m/s}$. (b) Results of an experiment to see if the membrane could be damaged by the AFM tip. The square, roughened patches in the upper and lower right (*arrows*) were created in the originally uniform layer by scanning at high force for an extended period. (c) Close-up view of a damaged region, showing the shape of the tear sites (*thick arrow*) and flaps of torn membrane (*thin arrow*).

AFM probe has apparently damaged some of the vesicles (*arrow*). The fact that the vesicle survives this damage intact, and that the furrow created by the tip is stable for subsequent imaging, suggests that under the present imaging conditions the vesicles are solid, multi-lamellar structures with little or no water in their centers. If so, their heights are consistent with ~ 10 to 20 bilayer lamellae per vesicle.

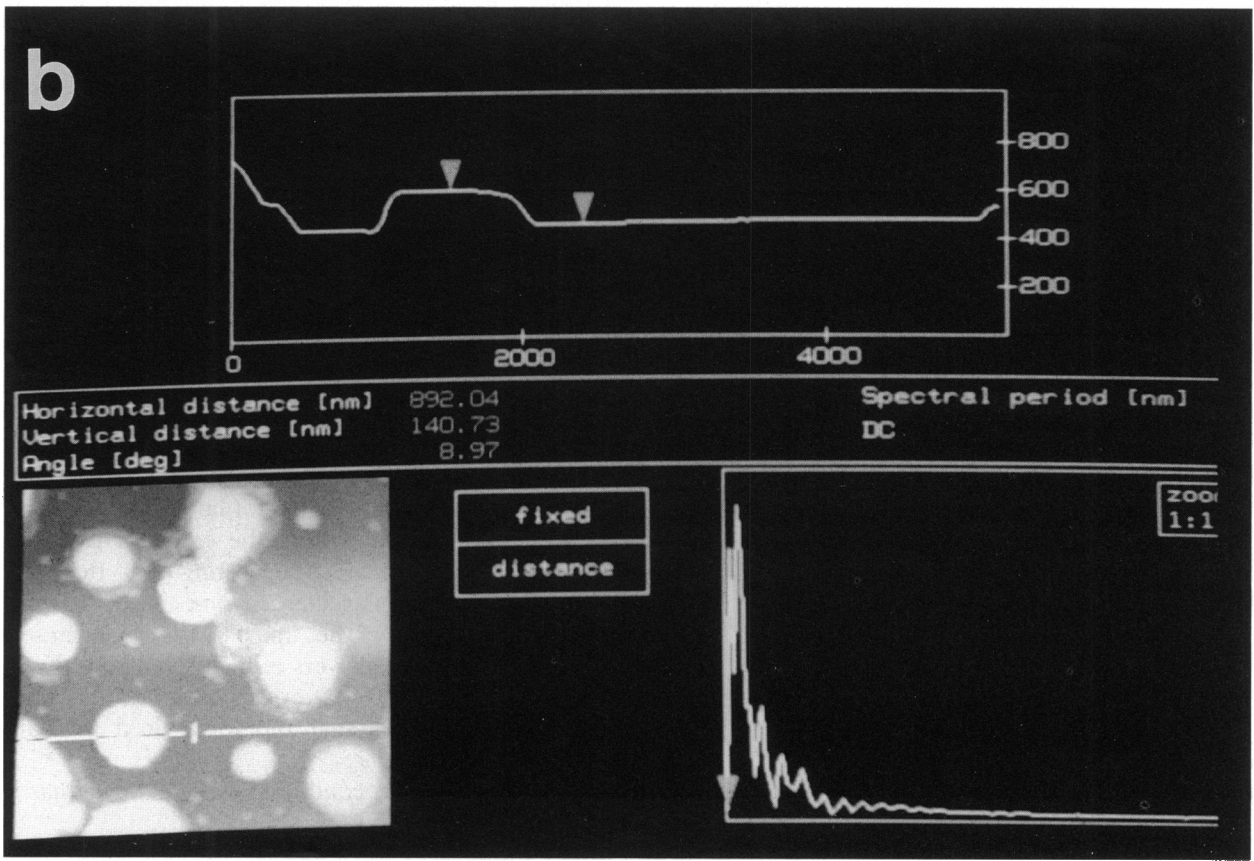
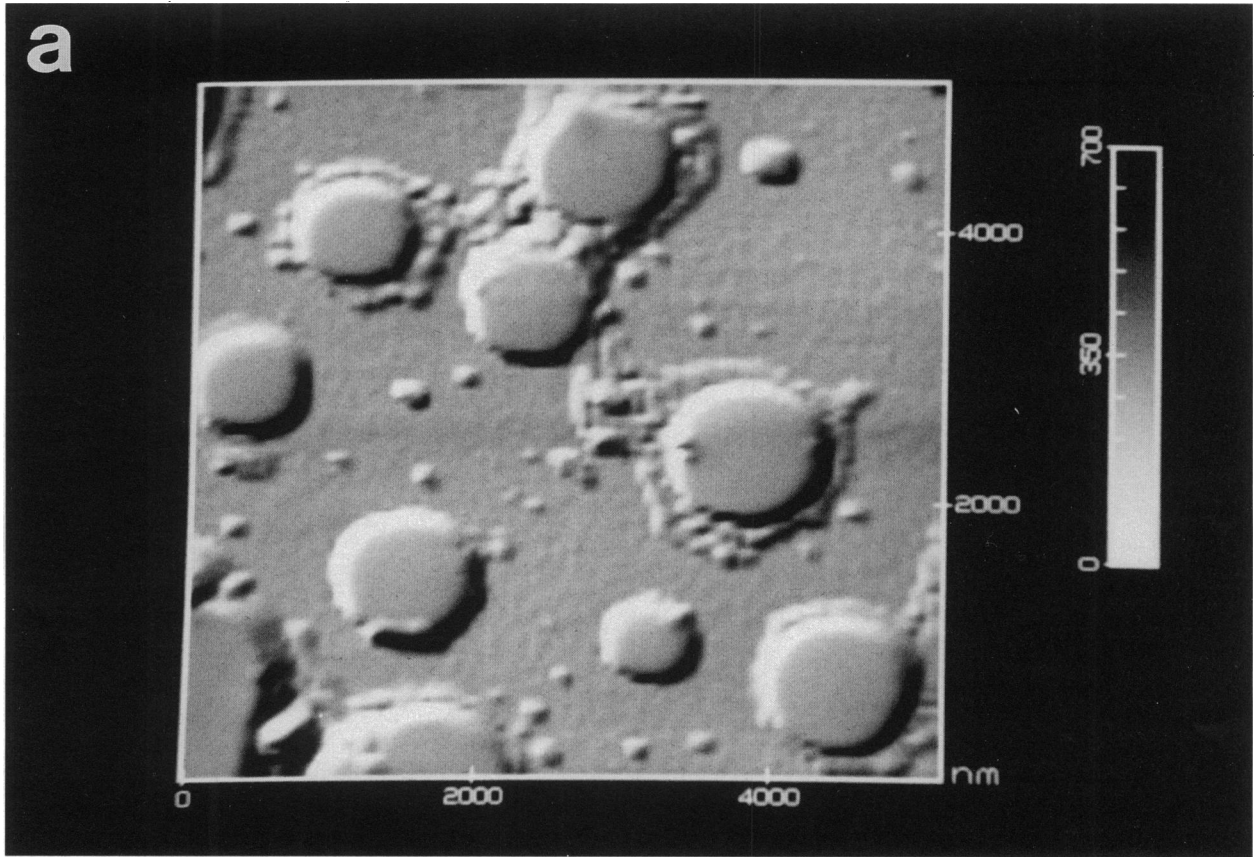
When these samples are rinsed in distilled water, the vesicles are washed away, and only circular "footprints" remain, where, we believe, the vesicles were once adsorbed. The footprints have no consistent thickness, and may be composed of fragments of torn lipid layers and salt crystals.

CONCLUSION

One of the main problems encountered in applying scanning probe microscopy to biological systems is their

tendency to be damaged or even entirely swept aside by forces between the tip and the sample (15). The tip-sample forces used in these experiments are fairly high, ~ 15 nN repulsive. Electron micrographs of the AFM cantilevers show the end of the best tips to be ~ 20 nm in diameter. If we therefore take the minimum area of tip sample contact to be $\sim 10 \times 10$ nm, the local pressure under the tip is of the order of 10^8 N/m². Despite these seemingly high pressures adsorbed bilayers show no evidence of damage under normal imaging conditions. In particular, there is no sign of large scale movements of the lipid molecules near the edges of isolated adsorbed bilayer domains, suggesting that the packing forces within the bilayer are strong enough to prevent much disruption by the tip. The damage caused by scanning adsorbed bilayers at high force, and the occasional damage to DPPE vesicles under normal imaging conditions, suggests that the force used is near the damage point.

Even under these conditions AFM imaging has been



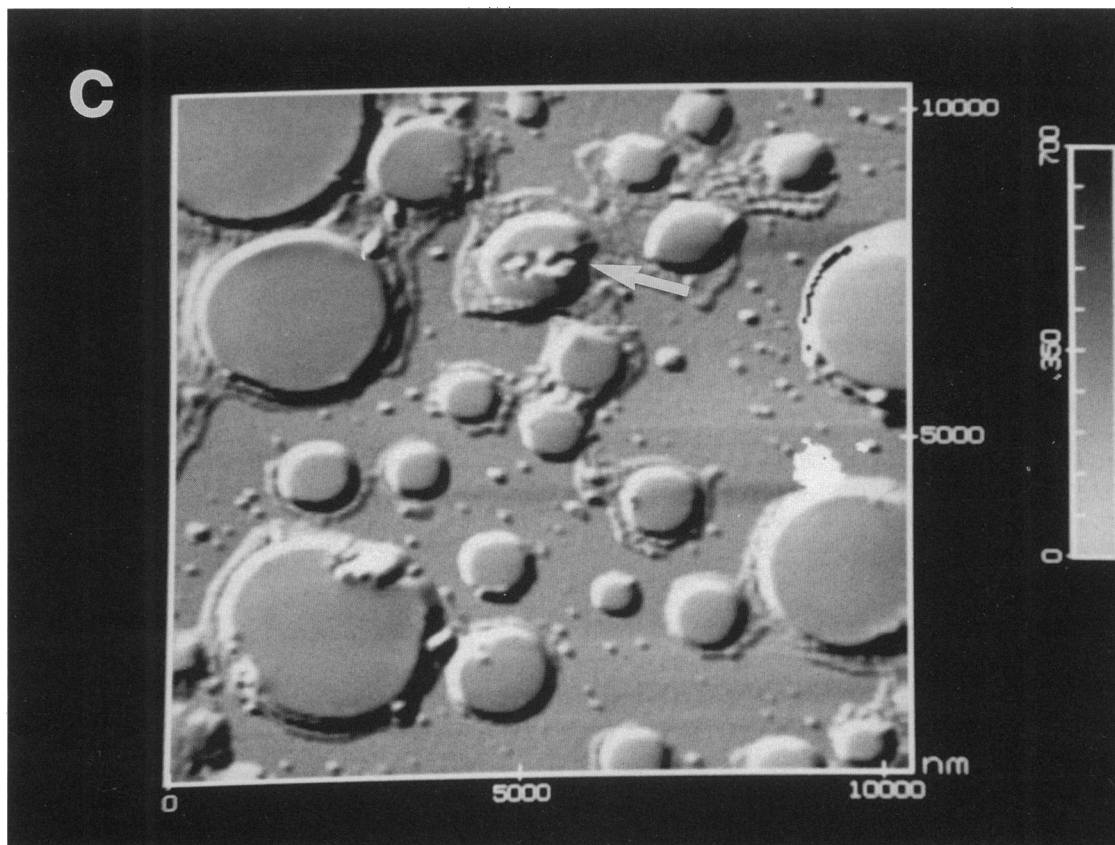


FIGURE 3 (a) AFM image of DPPE vesicles adsorbed on a mica substrate from an aged vesicle suspension. Each adsorbed vesicle is surrounded by salt crystals. Image processed by high pass filtering to enhance edges. Image taken in air, cantilever force constant ~ 0.6 N/m, net force ~ 15 nN, scan speed $13 \mu\text{m/s}$. (b) Cross-section of several vesicles showing their flattened shape. The height of the larger vesicles is $\sim 1,000$ to $2,000 \text{ \AA}$, consistent with a multilamellar structure containing ~ 10 to 20 lamellae. (c) AFM image of another DPPE sample showing a damaged vesicle (arrow). The survival of this damaged vesicle, and the stability of the damaged region suggest that the vesicles are made up of solid multilamellar lipid at the time of imaging, and do not contain hollow, water-filled centers.

quite reliable. Images very similar to those shown in Figs. 1–3 were obtained in 8 out of 11 experiments. In the unsuccessful cases the problem appears to be nonuniform deposition or otherwise damaged samples, not the imaging process itself. With care the applied force can be reduced to ~ 1 nN in this instrument (and possibly lower with improvements in instrumentation), which should improve reliability and decrease distortion and damage caused by the tip.

Supported membranes should therefore be capable of acting as well defined, physiologically-natural anchors for imaging membrane proteins. With slight changes in our deposition methods, one or more membrane proteins can be incorporated into supported bilayers at known concentrations (12), thus creating a simple artificial membrane system that can be investigated by AFM.

This work was supported by Research Allocations Committee, Biomedical Research Support grants, and Sandia-University Research Program grants to Dr. Keller.

Received for publication 9 April 1991 and in final form 9 August 1991.

REFERENCES

1. Diefenhofer, J., O. Epp, K. Miki, R. Huber, and H. Michel. 1984. X-ray structure analysis of a membrane protein: electron density map at 3 \AA resolution and a model of the chromophores of the photosynthetic reaction center from *rhodospseudomonas viridis*. *J. Mol. Biol.* 180:385–398.
2. Henderson, R., J. M. Baldwin, T. A. Ceska, F. Zemlin, E. Beckman, and K. H. Downing. 1990. Model for the structure of bacteriorhodopsin based on high-resolution electron cryomicroscopy. *J. Mol. Biol.* 213:899–929.
3. Binnig, G., H. Rohrer, Ch. Gerber, and E. Weibel. 1982. Surface studies by scanning tunneling microscopy. *Phys. Rev. Lett.* 49:57–61.
4. Albrecht, T. R., and C. F. Quate. Atomic resolution imaging of a nonconductor by atomic force microscopy. 1987. *J. Appl. Phys.* 62:2599–2602.

-
5. Drake, B., R. Sonnenfeld, J. Schneir, and P. K. Hansma. 1987. Scanning tunneling microscopy of processes at solid-liquid interfaces. *Surf. Sci.* 181:92-97.
 6. Gould, S. A. C., B. Drake, C. B. Prater, A. L. Weisenhorn, S. Manne, H. G. Hansma, P. K. Hansma, J. Massie, M. Longmire, V. Elings, B. D. Northern, B. Mukerjee, C. M. Peterson, W. Stoeckenius, T. R. Albrecht, and C. F. Quate. 1990. From atoms to integrated circuit chips, blood cells, and bacteria with the atomic force microscope. *J. Vac. Sci. Technol.* A8:369-373.
 7. Drake, B., C. B. Prater, A. L. Weisenhorn, S. A. C. Gould, T. R. Albrecht, C. F. Quate, D. S. Cannell, H. G. Hansma, and P. K. Hansma. 1989. Imaging crystals, polymers, and processes in water with the atomic force microscope. *Science (Wash. DC)*. 243:1586-1589.
 8. Hansma, P. K., and J. Tersoff. 1987. Scanning tunneling microscopy. *J. Appl. Phys.* 61:R1-R23.
 9. Worcester, D. L., R. G. Miller, and P. J. Bryant. 1988. Atomic force microscopy of purple membranes. *J. Microsc.* 152:817-821.
 - 9a. Worcester, D. L., H. S. Kim, R. G. Miller, and P. J. Bryant. 1990. Imaging bacteriorhodopsin lattices in purple membranes with atomic force microscopy. *J. Vac. Sci. Technol.* A8:403-405.
 10. Butt, H.-J., K. H. Downing, and P. K. Hansma. 1990. Imaging the membrane protein bacteriorhodopsin with the atomic force microscope. *Biophys. J.* 58:1473-1480.
 11. Egger, M., F. Ohnesorge, A. L. Weisenhorn, S. P. Heyn, B. Drake, C. B. Prater, S. A. C. Gould, P. K. Hansma, and H. E. Gaub. 1990. Wet lipid-protein membrane images at submolecular resolution by atomic force microscopy. *J. Struct. Biol.* 103:89-94.
 12. McConnell, H. M., T. H. Watts, R. M. Weiss, and A. A. Brian. 1986. Supported planar membranes in studies of cell-cell recognition in the immune system. *Biochim. Biophys. Acta.* 864:95-106.
 13. Brian, A. A., and H. M. McConnell. 1984. Allogenic stimulation of cytotoxic T cells by supported planar membranes. *Proc. Natl. Acad. Sci. USA.* 81:6159-6163.
 14. Sackmann, E., 1983. Physical foundations of the molecular organization and dynamics of membranes. In *Biophysics*. Walter Hoppe, Wolfgang Lohmann, Hubert Markl, and Hubert Zeigler, editors, Springer-Verlag, New York. 425-457.
 15. Keller, D., C. Bustamante, and R. Keller. 1989. Imaging of single uncoated DNA molecules by scanning tunneling microscopy. *Proc. Natl. Acad. Sci. USA.* 86:5356-5360.